FLEXURAL-TORSIONAL VIBRATIONS OF THIN-WALLED BEAMS*

Marzio Falco** and Michele Gasparetto***

SOMMARIO: In questo lavoro si espone un metodo di calcolo basato sulle matrici di trasferimento per determinare i modi principali di vibrare di travi a T corrispondenti a deformate flesso-torsionali.

Vengono esposti i risultati ottenuti dal calcolo per differenti condizioni di vincolo, mettendo in luce l'influenza del vincolo stesso sulle pulsazioni proprie e relative deformate.

Si espongono le ricerche sperimentali eseguite su travi a T eccitate in risonanza e le si confrontano con i risultati di calcolo.

SUMMARY: Description of a method of calculation based on trasfer matrices for determining the principal modes of vibrations of T beams taking into account torsional and flexional coupling.

The results obtained from the calculation for different constraint conditions are compared and the influence of the constraint on the own frequencies and relative deflection configurations evidenced.

The experimental studies carried out on T beams excited in resonance are described and compared with those of calculation.

1. Introduction.

The computation of the transverse natural frequencies of thin-walled beams of constant section, such as T or L beams, without taking flexural-torsional coupling into account is held to be generally valid if the flexural and torsional frequencies are sufficiently apart and if the distance between the gravity center and the shear center is sufficiently small compared to the transverse dimension of the beam.

In the context of a study conducted at the Institute of Machine Mechanics of the Milan Polytechnic on aeroelastic problems connected with vibrations of T and L elements of lattice structures it emerged that, even in cases in which the above conditions were thought to have been satisfied, when flexural-torsional coupling was neglected, the calculated results differed considerably from the experimental results.

It was also noted that the constraints exert considerable influence on flexural-torsional coupling.

In many problems it is essential to know the value of the natural frequencies and of the corresponding deflection configurations fairly accurately; one example is the phenomenon of aerodynamic instability and of self-excited vibrations through the detaching of vortices [2]. We therefore decided to devise a method of calculation that would take account of flexural-torsional coupling for various constraint conditions and to find out whether this method would yield results in agreement with those obtained experimentally.

Our analysis concentrated on T beams but the conclusions obtained can be extended to other types of sections which, like T and L beams, do not present warping rigidity.

2. Method of calculation.

Referring to the theory of Vlasov [1] for thin-walled open beams consisting of plates connected along a line, this line is taken as the locus of the shear centers, and for the beams under study the torsional warping to buckling is zero and hence the cross sections of the beam remain flat and undeformed.

The displacements y and z of the shear center in the direction indicated in Figure 1 and the rotation ϑ of the section with respect to the shear center are taken as independent variables.

In this study we consider T beams, or equal-sided L beams, in which the shear center lies on the main axis of inertia (y), coincident with the axis of symmetry of the section. In this way vibrations in the plane containing the y axis are purely flexural.

The torsional vibrations are thus only coupled with the flexural vibrations in the plane containing the z axis.

With reference to Fig. 1 the notation is as follows:

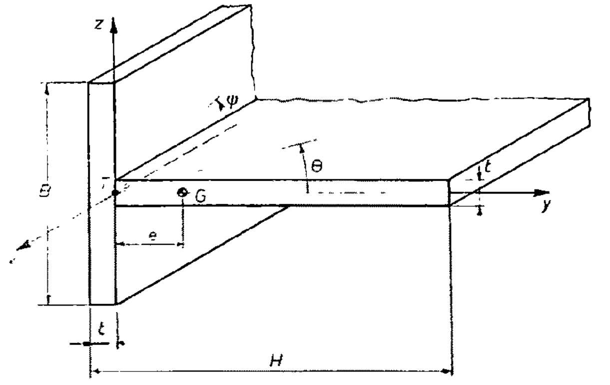

Fig. 1

* The Institute of Applied Mechanics Milan Polytechnic received a CNR subsidy to carry out this research.

** Istituto di Meccanica Applicata alle Macchine, Università di Pavia.

*** Istituto di Meccanica Applicata alle Macchine, Politecnico di Milano.

e = distance of shear center T from gravity center G
m = mass per unit length of the beam
EI_y = flexural rigidity of the beam with respect to axis y
EI_z = flexural rigidity of the beam with respect to axis z
GJ = torsional rigidity of the beam
ϱ = radius of gyration of the section with respect to the center-of-gravity axis parallel to x
L = beam length
z = shear center displacement
z_G = center-of-gravity displacement
ϑ = torsional rotation of the section
ψ = flexural rotation of the beam axis
T = shear
M = bending moment
M_t = twisting moment.

The study of the beam may be approached by solving the differential equations that are obtained by imposing the equilibrium of an infinitesimal element of the beam

$$EI_z\frac{\partial^4 y}{\partial x^4} - mI_z\frac{\partial^4 y}{\partial x^2 \partial t^2} + m\frac{\partial^2 y}{\partial t^2} = 0$$

$$EI_y\frac{\partial^4 z}{\partial x^4} - mI_y\frac{\partial^4 z}{\partial x^2 \partial t^2} + m\frac{\partial^2 z}{\partial t^2} + em\frac{\partial^2 \vartheta}{\partial t^2} = 0 \qquad (2.1)$$

$$-GJ\frac{\partial^2 \vartheta}{\partial x^2} + m\varrho^2\frac{\partial^2 \vartheta}{\partial t^2} + me^2\frac{\partial^2 \vartheta}{\partial t^2} + em\frac{\partial^2 z}{\partial t^2} = 0\,.$$

the system. In the second equation the second term is generally neglected [3] since it is very small.

The integration of this system of equations with partial derivatives has been carried out but it presented considerable analytic and numeric difficulties.

It was therefore preferred to schematise the beam with an elastic system (Figure 2) consisting of an ideal beam, devoid of mass, with n concentrated and equidistant masses. The ideal beam has the same elastic characteristics as the beam under study and every mass is equivalent from the inertial point of view (m_i, ϱ) to the section of beam between two successive masses, the section being conceived as rigid.

The greater the number of subdivisions, the more approximate is this schematisation.

This model is particularly suitable for study with the transfer matrix method.

3. Transfer matrix method.

This method [4], [5], [6] envisages point matrices $[P]$ which transfer the characteristic quantities from left to right of the generic mass and field matrices $[C]$ which transfer the same quantities from left to right of the generic elastic section of the length of $\Delta_x = L/(n+1)$. Knowing these matrices, we can obtain the global matrix $[T]$ which

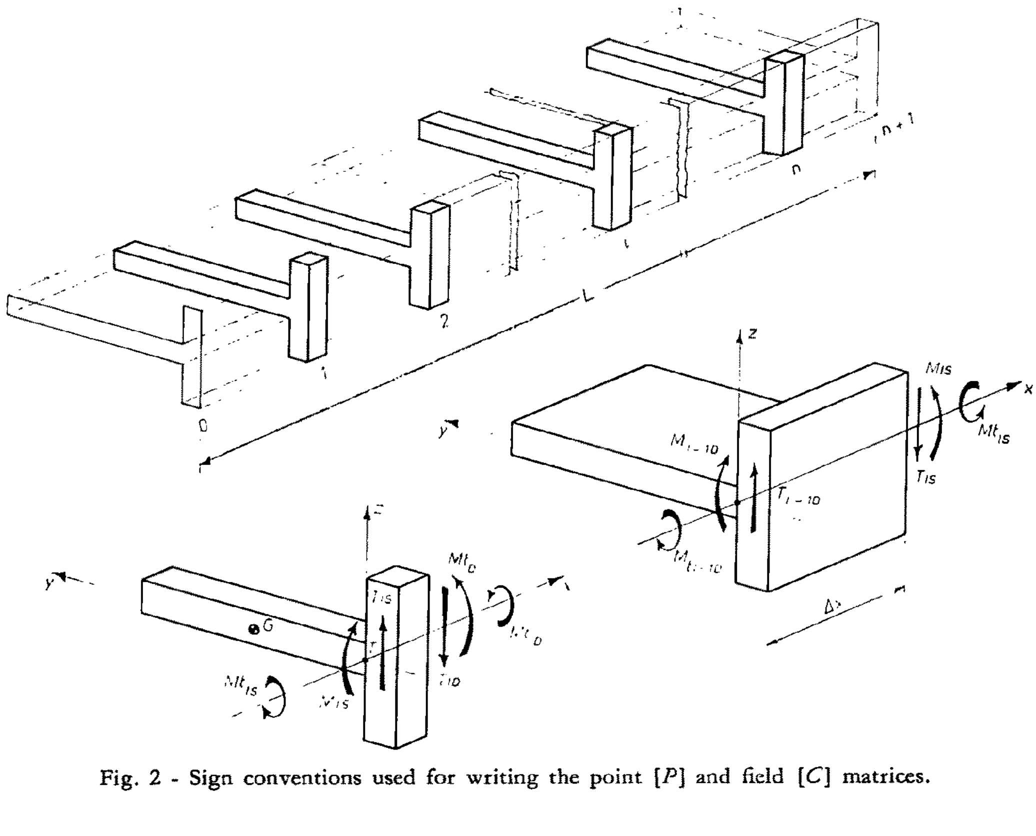

Fig. 2 - Sign conventions used for writing the point $[P]$ and field $[C]$ matrices.

Of the above three differential equations the first and second represent the dynamic equilibrium of the beam element in the direction of axes y and z respectively and the third the equilibrium on rotation about axis x. In this last equation the 4th order differential terms in ϑ do not appear since the warping constant is zero.

We shall be concerned with the last two equations of transfers the characteristic quantities from end to end of the beam.

The quantities that completely determine the behavior of a generic section are: z, ψ, ϑ, T, M, M_t. These quantities are collected in the state vector of the section considered

$$\bar{Y} = |z,\ \ \psi,\ \ M,\ \ T,\ \ \vartheta,\ \ M_t|$$

To determine the point matrix relating to the i-th mass $m_i = m\Delta x$ we write the relations between the state vectors $\bar{Y}_{iS}$ and $\bar{Y}_{iD}$, having indicated by index i_S all the quantities relating to the section immediately to the left of the i-th mass and by index i_D those to its right (Fig. 2).

Assuming that the sections remain rigid and that the vibrations are sinusoidal in time with frequency ω, the acceleration is

$$\ddot{z}_{Gi} = -(z_i + e\vartheta_i)\omega^2$$

and hence for the equilibrium and congruence the following equations may be written

$$z_{iD} = z_{iS}\,, \qquad \psi_{iD} = \psi_{iS}\,, \qquad M_{iD} = M_{iS}$$

$$T_{iD} = T_{iS} + m_i\omega^2(z_i + e\vartheta_i)\,, \qquad \vartheta_{iD} = \vartheta_{iS}$$

$$M_{tiD} = M_{tiS} - m_i\varrho^2\omega^2\vartheta_i - m_i\omega^2 e(z_i + e\vartheta_i)$$

These relations, suitably ordered, are synthesised in matrix form:

$$\bar{Y}_{iD} = [P_i]\bar{Y}_{iS}$$

in which $[P_i]$ is the point matrix of the i-th mass and is equal to

$$[P_i] = \begin{bmatrix} 1 & 0 & 0 & 0 & 0 & 0 \\ 0 & 1 & 0 & 0 & 0 & 0 \\ 0 & 0 & 1 & 0 & 0 & 0 \\ m_i\omega^2 & 0 & 0 & 1 & m_i\omega^2 & 0 \\ 0 & 0 & 0 & 0 & 1 & 0 \\ -m_ie\omega^2 & 0 & 0 & 0 & -m_i\omega^2(e^2+\varrho^2) & 1 \end{bmatrix}$$

Similarly we will now consider the elastic segment between the $i-1$ and the i-th mass. In the small deformation range since, with the sign conventions used

$$T = \frac{dM}{dx} \qquad M = EI_y\frac{d\psi}{dx} \qquad \psi = \frac{dz}{dx}$$

we obtain the relation between the state vectors Y_{i-1D} and Y_{iS}

$$T_{iS} = T_{i-1D}$$

$$M_{iS} = M_{i-1D} + T_{i-1D}\cdot\Delta x$$

$$\psi_{iS} = \psi_{i-1D} + \frac{\Delta x}{EI_y}\cdot M_{i-1D} + \frac{(\Delta x)^2}{2EI_y}T_{i-1D}$$

$$z_{iS} = z_{i-1D} + \psi_{i-1D}\Delta x + \frac{(\Delta x)^2}{2EI_y}\cdot M_{i-1D} + \frac{(\Delta x)^3}{6EI_y}\cdot T_{i-D}$$

$$M_{tiS} = M_{ti-1D}$$

$$\vartheta_{iS} = \vartheta_{i-1D} + \frac{\Delta x}{GJ}M_{ti-1D}$$

and hence

$$\bar{Y}_{iS} = [C_i]\bar{Y}_{i-1D}$$

where the field matrix of the i-th segment is

$$[C_i] = \begin{bmatrix} 1 & \Delta x & \frac{(\Delta x)^2}{2EI_y} & \frac{(\Delta x)^3}{6EI_y} & 0 & 0 \\ 0 & 1 & \frac{\Delta x}{EI_y} & \frac{(\Delta x)^2}{2EI_y} & 0 & 0 \\ 0 & 0 & 1 & \Delta x & 0 & 0 \\ 0 & 0 & 0 & 1 & 0 & 0 \\ 0 & 0 & 0 & 0 & 1 & \frac{\Delta x}{GJ} \\ 0 & 0 & 0 & 0 & 0 & 1 \end{bmatrix}$$

From the product of the field matrix and the point matrix we obtain the matrix $[PC_i]$ which relates the state vector on the right of the i-th mass to that on the right of the $i-1$-th

$$\bar{Y}_{iD} = [PC_i]\bar{Y}_{i-1D} \qquad [PC_i] = [P_i]\cdot[C_i]$$

The transfer matrix that permits transition from the state vector of the initial section Y_0 of the beam to the last Y_{n+1} is defined by the matrix relation

$$\bar{Y}_{n+1} = [T]\cdot\bar{Y}_0 \tag{3.2}$$

is a function of the frequency ω and is equal to

$$T = [C_{n+1}]\,[PC_n]\cdots[PC_i]\cdots[PC_2]\,[PC_1]$$

Relation (3.2) represents a system of six equations with six unknowns, three in $\bar{Y}_{n+1}$ and three in $\bar{Y}_0$.

Indeed, of the 12 boundary conditions three per side are known. They are zero in the case of non yielding constraints. For example, in the case of hinge $z = 0$; $M = 0$; $M_t = 0$ and the state vector is

$$\bar{Y} = |0,\ \psi,\ 0,\ T,\ \vartheta,\ 0| \tag{3.3}$$

In the case of clamp $z = 0$, $\psi = 0$, $\vartheta = 0$ and hence

$$\bar{Y} = |0,\ 0,\ M,\ T,\ 0,\ M_t| \tag{3.4}$$

From the system we can thus isolate three homogeneous equations with only three unknowns which appear in $\bar{Y}_0$.

The values of ω that zeroes the determinant of the coefficients of the three homogeneous equations are the natural frequencies of the beam. The coefficients in question are the elements of the minor isolated from transfer matrix $[T]$ by eliminating the columns corresponding to the zeroes of $\bar{Y}_0$ and the lines corresponding to the unknown values of $\bar{Y}_{n+1}$.

$$
[PC_i] = \begin{bmatrix}
1 & \Delta x & \dfrac{(\Delta x)^2}{2EI_y} & \dfrac{(\Delta x)^3}{6EI_y} & 0 & 0 \\
0 & 1 & \dfrac{\Delta x}{EI_y} & \dfrac{(\Delta x)^2}{2EI_y} & 0 & 0 \\
0 & 0 & 1 & \Delta x & 0 & 0 \\
m_i\omega^2 & m_i\omega^2 \Delta x & m_i\omega^2 \dfrac{(\Delta x)^2}{2EI_y} & 1 + m_i\omega^2 \dfrac{(\Delta x)^3}{6EI_y} & m_i\omega^2 e & m_i\omega^2 e \dfrac{\Delta x}{GJ} \\
0 & 0 & 0 & 0 & 1 & \dfrac{\Delta x}{GJ} \\
-m_i\omega^2 \cdot e & -m_i\omega^2 \Delta x \cdot e & -m_i\omega^2 \dfrac{(\Delta x)^2}{2EI_y} \cdot e & -m_i\omega^2 \cdot e \dfrac{(\Delta x)^3}{6EI_y} & -m_i\omega^2 \cdot (e^2 + \varrho^2) & 1 - (e^2 + \varrho^2) \dfrac{\Delta x \cdot m_i \cdot \omega^2}{GJ}
\end{bmatrix}
$$

For example, in the case of a beam hinged at the ends the minor considered is

$$
[MT] = \begin{vmatrix} T_{12} & T_{14} & T_{15} \\ T_{32} & T_{34} & T_{35} \\ T_{62} & T_{64} & T_{65} \end{vmatrix}
$$

In the case of clamps

$$
[MT] = \begin{vmatrix} T_{13} & T_{14} & T_{16} \\ T_{23} & T_{24} & T_{26} \\ T_{53} & T_{54} & T_{56} \end{vmatrix}
$$

To obtain the ω values that zeroes the determinant of the above minor we used an iterative numeric method consisting in imposing successive values of ω and arriving at the frequency by interpolation.

For each value of the natural frequencies ω we obtain from (3.2) the six unknown boundary conditions up to an arbitrary multiplying constant.

Multiplying the state vector at the boundary by the point and field matrices we obtain the state vectors all along the beam and we can therefore plot both the deformations and the internal stresses of the beam for the various natural frequencies.

All these calculations can easily be done on a computer. T beams of different sections and lengths were studied and the relevant calculations done on the UNIVAC 1108 computer. The results are given in the following paragraphs.

4. Experimental tests.

The hypotheses and schematisations of the method of calculation used were then laboratory tested by measuring the natural frequencies and relative deformations of beams excited in resonance, using types of T beams commonly used in lattice structures (Fig. 3).

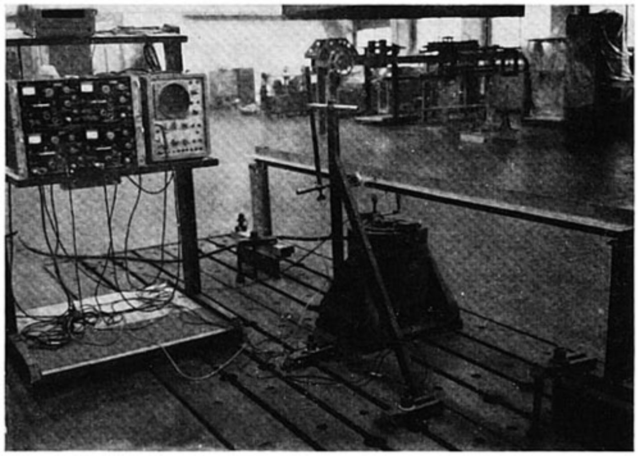

Fig. 3 - View of the beam, of the excitation system and of part of the instrumentation used for the experimental tests.

The beams were constrained at the ends to two very rigid uprights by pairs of bolts fixed to the core or to the flange (Fig. 4).

These constraints are the ones most commonly used in practice. The beams were excited by means of a dynamometric device constrained on one side to the beam and on

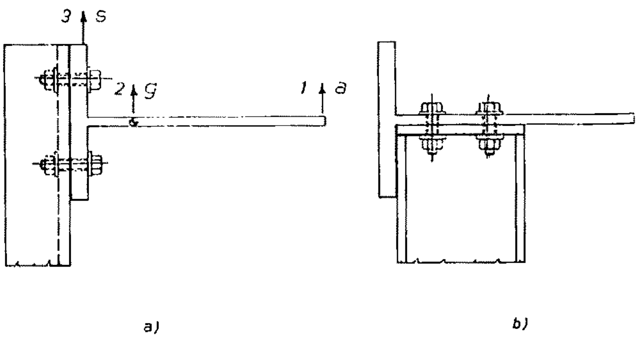

Fig. 4 - The constraints as they were in the experimental tests: *a*) flexural-torsional clamp; *b*) torsional clamp and flexural hinge (half-hinge).

the other to an *MB* Electronics CF6/190 electromagnetic shaker controlled by a B & K 1016 oscillator.

The dynamometric device was based on an elastic system (Fig. 5) whose strains, and hence the force imparted, were measured by electric strain gauges. The device consisted of a beam acting as a constant flexibility spring, permitting easy regulation of the force imparted. The dynamometer was connected to a Vibrometer 200/8-A station.

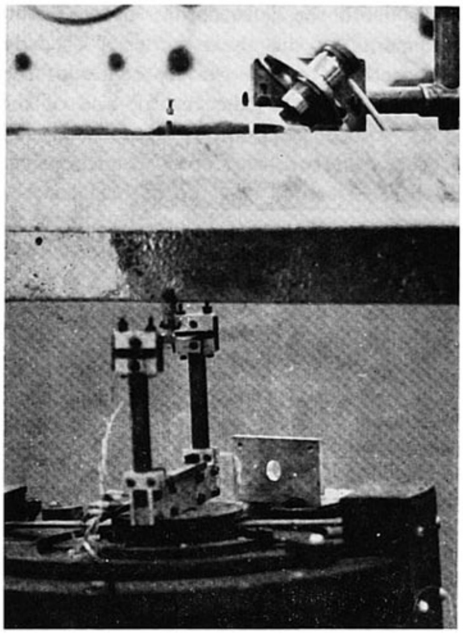

Fig. 5 - View of the dynamometer and of the pick-up used for checking the resonance.

The beam deflections were recorded by Philips PR 9310/01 inductive displacement pick-ups connected to Vibrometer measuring decks and Kistler accelerometers with Vibrometer TA-2/C piezoamplifiers with TP 20/A. The signals of these pick-ups were visualised on an oscilloscope and recorded by a Gailleo RSJ14 galvanometric recorder.

The resonance was controlled on a second oscilloscope to which were sent the signals of the dynamometer, which measured the force imparted to the beam, and of the pick-up, which measured the displacement of the application point of the force. The frequency of the vibration was checked with an H. P. type 3734 A frequency meter.

Experimental tests were not always feasible because of the presence, as will be shown later (Table I), of very close natural frequencies; continuous control of the resonance frequency was thus essential for the correct recording of the quantities under study. Not all the natural modes could be excited easily, again because of very close natural frequencies.

5. Theoretical results and experimental checks.

The calculations with the method described earlier were done in order to obtain natural frequencies and relative deformations with the following constraint conditions:

a) flexural-torsional clamp (clamp).

b) flexural hinge and torsional joint (half-hinge).

TABLE I

T Beam H = 165 mm B = 100 mm t = 4,5 mm					
Length l [m]	ω_t [r/s] Torsional	ω_{fc} [r/s] Flexural (hinge)	ω_{fi} [r/s] Flexural (clamp)	ω [r/s] Flexural-torsional (half-hinge)	ω [r/s] Flexural-torsional (clamp)
l = 3m	148	99	228	82,81 C_1 I ×	109,14 i_1 I ×
	296	397	722	184,6 C_3 I	224,64 i_3 II ×
				213,7 C_2 II	303,4 I f + III t
l = 5m	88,6	35,6	82	33,7 C_1 I f	58 i_1 I ×
	177	141	225	97,9 C_3 I	126,8 i_2 I
	266	320	440	109,6 C_2 II ×	126,9 i_3 II ×
				187,8 C_4 III	200,8 i_4
				240 C_5 II	259,7 i_5
					332,3 II f - IV t
l = 6m	74	24,8	57	23,9 C_1 I f	44,5 i_1 I ×
	148	99,5	181	80 C_3 I	95 i_2 I
	222	222	306	82,8 C_2 II ×	101,4 i_3 II ×
				149,4 C_4 III ×	163 i_4
l = 6,6m				18,9 C_1 I f	38,4 i_1 I ×
	67,1	20,5	46,8	70,77 C_2 II ×	83,48 i_2 I
	134,2	82,1	129,5	72,17 C_3 I	89,5 i_3 II ×
	201,3	184,5	25[illegible]	131,5 C_4 II ×	146,5 i_4
	258,4	300		152,1 C_5 I	183 i_5
				190 C_6 III	217 i_6
l = 7m	63,5	18	42	17,7 C_1 I f	34,96 i_1 I ×
	127	72,[illegible]	[illegible]	64 C_2 II ×	76,96 i_2 I
	192	15[illegible]	[illegible]	67,8 [illegible] I	82,56 i_3 II ×
				121,1 [illegible] II ×	136,44 [illegible]
				150 [illegible]	
l = 8m	55,4	[illegible]	31,8	13,7 C_1 I f	28,3 i_1 I f
	111	55	88	[illegible] C_2 [illegible]	65 i_2 I
	[illegible]	12[illegible]	[illegible]	58,9 C_3 I	68,9 i_3 II ×
		[illegible]		99,5 [illegible] II ×	116,5 [illegible]
				127,1 C_5 II	140,9 i_5
				149,4 [illegible] III	

TABLE II

T Beam H = 165 mm B = 100 mm l = 5 m					
Thickness t [mm]	ω_t [r/s] Torsional	ω_{fc} [r/s] Flexural (hinge)	ω_{fi} [r/s] Flexural (clamp)	ω [r/s] Flexural-torsional (half-hinge)	ω [r/s] Flexural-torsional (clamp)
t = 1,5mm	31,5	35,8	80	20,48 I ×	22,21 I t
	62,2	143	222	44,08 II	44,7 II t
				52,5 C_3 I	66,69 III t
				66,76 C_4 III	89,06 IV t
					109 I f + IV t
t = 2mm	39,7	35,8	80	25,22 I ×	29,32 I t
	79,4	143	222	57,05 C_3 I	59,43 II t
				57,93 C_2 II	87,96 III t
				88,68 C_4 II t	113 I f + III t
t = 2,5mm	50,6	35,8	80	28,53 I ×	36,11 I ×
	10[illegible]2	143	222	63,29 C_3 I	73,91 II t
				70,9 C_2 II	104,85 I f + III t
				110,16 C_4 III	120,7 i_4
t = 3mm	59	35,8	80	30,70 C_1 I ×	42,5 I
	118	143	222	70,86 C_3 I	88,03 II
				82,7 C_2 II	112,3 I f + III t
				131,01 C_4 II	138,2 i_4
t = 4,5mm	88,6	35,6	82	33,7 C_1 I f	58 i_1 I ×
	177	141	225	97,9 C_3 I	126,8 i_2
				109,6 C_2 II ×	126,98 i_3 II ×
t = 6mm	124	35,6	82	34,86 C_1 I ×	67,81 i_1 I ×
	248	141	225	124,65 C_2 II ×	146,87 i_2 I
				127,77 C_3 I	158,43 i_3 II ×
				232,66 C_4 III ×	259,25 i_4

These are the constraints that approximate closest to the real constraints, which were used in the experimental tests (Fig. 5). Indeed, assuming that the sections remain flat and undeformed, the constraint on the core, virtually coincident with the neutral axis for the flexions considered, behaves like a flexural hinge, whereas the constraint on the flange prevents these flexions. With regard to torsion, both types of constraint allow no rotation ϑ and so may be regarded as torsional joints.

The boundary conditions corresponding to the perfect clamp were given in (3.4); those for the half-hinge are $z = 0$; $M = 0$; $\vartheta = 0$. It follows that the state vector is:

$$\bar{Y} = |0,\ \psi,\ 0,\ T,\ 0,\ M_t|$$

We give in tables 1 and 2 the results for steel T beams of various lengths and thicknesses having the following dimensions (see Fig. 1) $H = 165$ mm $B = 100$ mm.

For T beam of length $L = 6.6$ m and $t = 4.5$ mm we give the natural frequencies and corresponding deflections calculated theoretically, compared with the corresponding experimental measurements: in Fig. 6 those for the case of the clamp and in Fig. 7 those for the half-hinge case.

For the convenience of subsequent exposition each deflections is marked with an identification initial. Since the calculated deflections are defined up to an arbitrary multiplying constant, the experimental and theoretical amplitudes are referred to unit amplitude at the antinode .To define the deformations of the beam we give the displacements of the shear center ("*s*" experimental and "3" theoretical), of the gravity center of the section ("*g*" experimental and "2" theoretical) and of the end of the core ("*a*" experimental and "1" theoretical). The tables give the natural flexural-torsional frequencies calculated by the method described and the natural frequencies for pure flexion and torsion for beams having the same H and B: table 1 for different lengths and equal thicknessn and table 2 for equal length and different thicknesses. To aid identification of the vibrating modes we give alongside the natural flexural-torsional frequencies the sign corre-

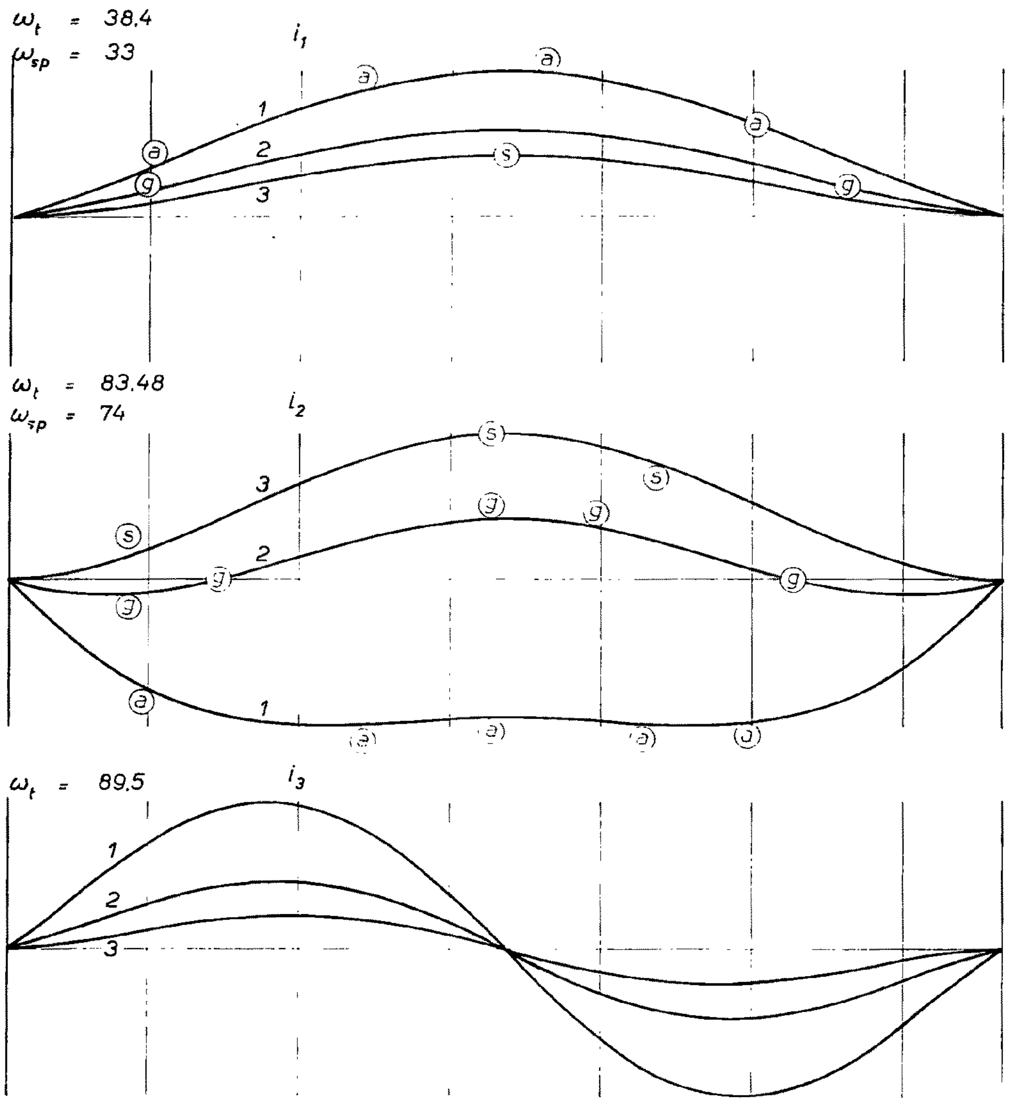

Fig. 6 - Calculated and experimental deflections of the T beam having $H = 100$ mm, $B = 165$ mm, $t = 4.5$ mm, $L = 6.6$ m, clamped at the ends; *s*, *g*, *a* are the experimental amplitudes and 1, 2, 3 the theoretical amplitudes of vibration of the corresponding points of fig. 4*a*.

ponding to the type of deflection shown in figs. 6 and 7 and also the number of the nearest pure flexural or torsional mode and, with an asterisk, the mean position of the center of torsion. The natural frequencies of pure flexion are calculated for clamp-clamp and for hinge-hinge at the ends and the pure torsion frequencies are calculated for clamp-clamp.

In the half-hinge case it will be noted (Fig. 7) that the torsion center of the various sections lies on a straight line parallel to axis x. Conversely, in the clamps case the torsion center does not lie on a straight line; there are vibrating modes in which some sections translate and others rotate and so for this type of constraint we give in Fig. 8 the position of the torsion center for the various modes of vibrating whose deformations are given in Fig. 6.

From the results it will be noted that the behavior of the beam for the first vibrating modes depends mainly on the ratio between the calculated natural frequency for pure flexion ω_f and the calculated frequency for pure torsion ω_t. Three fundamental cases may be distinguished:

a) Natural flexural frequency $\omega_f \ll \omega_t$

b) Natural flexural frequency $\omega_f \gg \omega_t$

c) Natural flexural frequency comparable with natural torsional frequency.

In case *a*) while the first mode of vibrating is flexural with a frequency virtually coinciding with ω_f, there is no comparable pure torsional mode. The mainly torsional mode, although having a natural frequency very close (slightly greater) to ω_t, has its torsion center virtually coincident with the gravity center of the section. Examples of this situation may be found in Table 1 when considering the torsional modes of beams, with half hinges at the ends, for L values for which the ω_f values are much smaller than ω_t.

Examples of case *b*) may be seen in table 2 in the column showing the flexural torsional modes of clamped beams relating to thicknesses for which ω_f if much greater than ω_t. In this case the first mode of vibrating is purely torsional about the shear center, but with a frequency appreciably lower than ω_t. The first mode of vibrating with an appreciable flexural component has a decidedly higher natural frequency than that of pure flexion.

In case *c*), that is when ω_f and ω_t are comparable, the modes of vibrating are no longer easily schematised. There

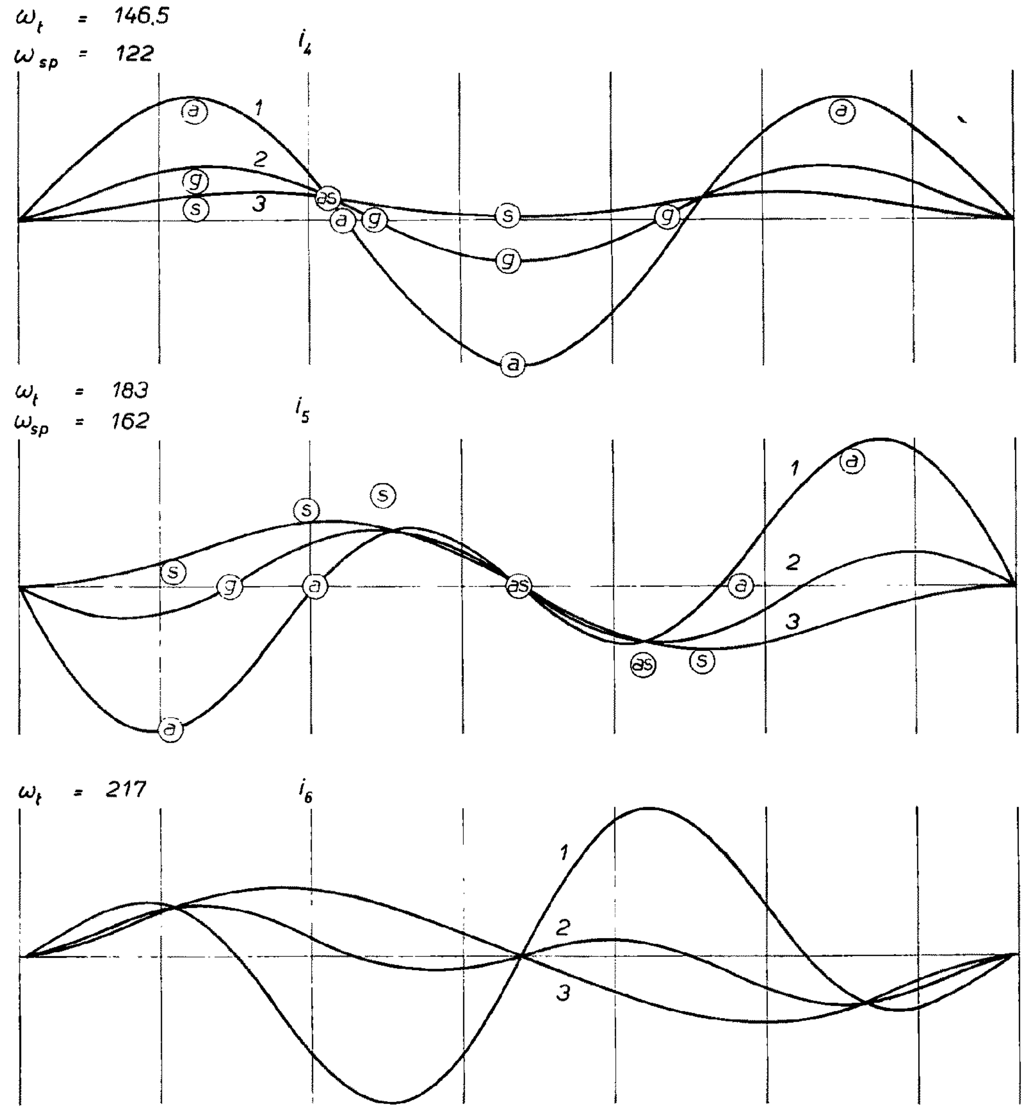

Fig. 6*b*

are numerous examples of this situation in tables 1 and 2 for the first modes of vibrating and even more for the subsequent modes in which the corresponding natural frequencies ω_f and ω_t are always comparable. For the first frequencies, when ω_f is greater than ω_t, the first of the flexural torsional modes with a distinct flexural component has a higher natural frequency than the first pure flexural

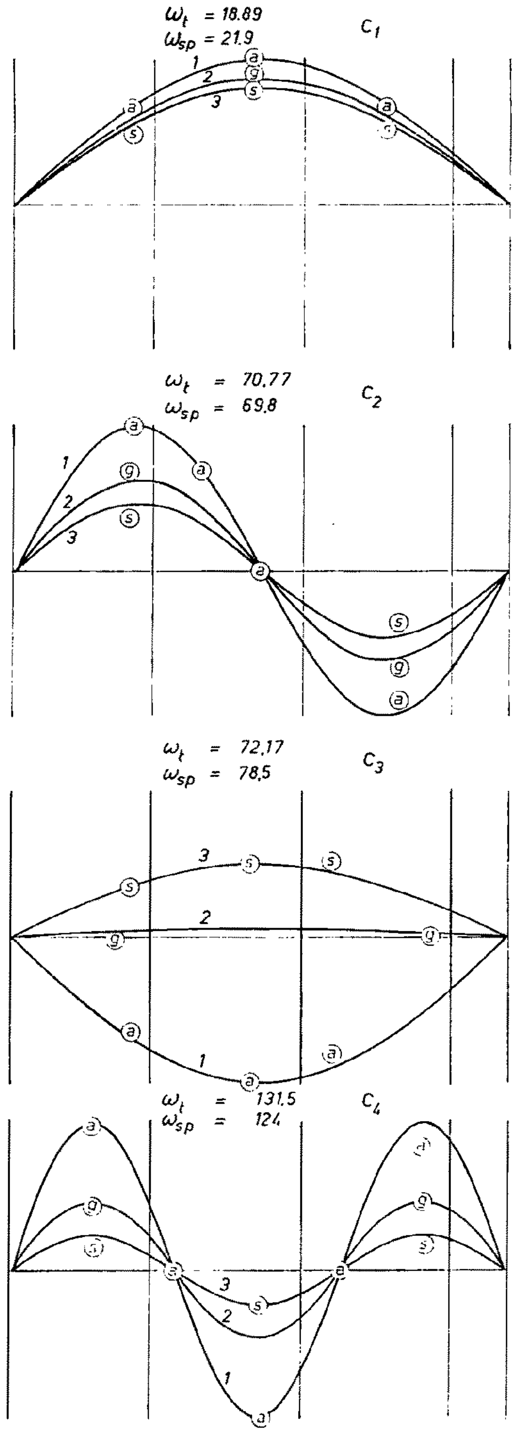

Fig. 7 - Calculated and experimental deflections of the T beam having $H = 100$ mm, $B = 165$ mm, $t = 4.5$ mm, $L = 6.6$ m, with torsional clamp and flexural hinge at the ends; s, g, a are the experimental amplitudes and 1, 2, 3 the theoretical amplitudes of vibration of the corresponding points of fig. 4*a*.

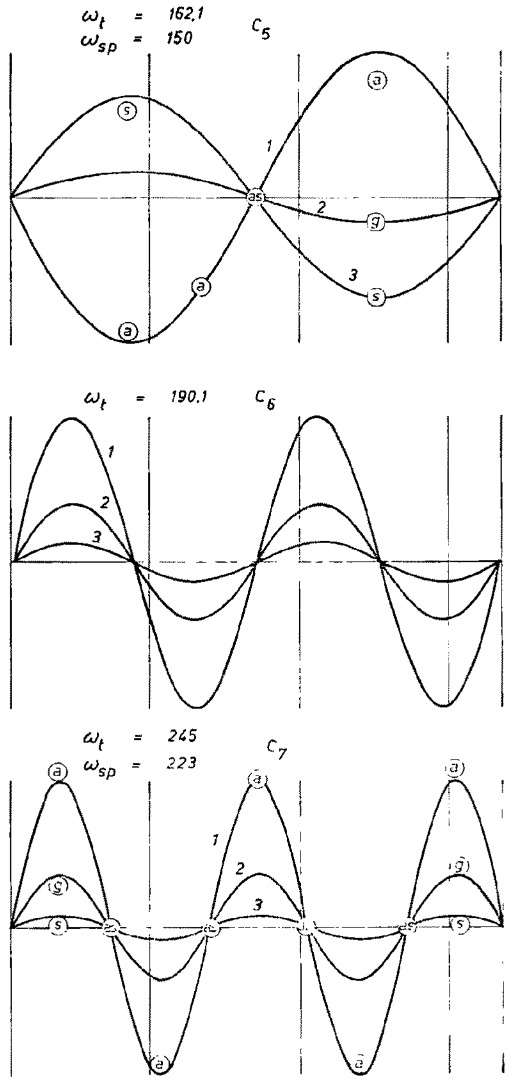

Fig. 7*b*

frequency, whereas the mainly torsional mode has a natural frequency lower than ω_t.

Given the great importance of the ratio between the pure flexural and pure torsional frequencies, for the thicknesses and lengths of the beams commonly used in lattice structures, the constraint conditions assume decisive importance since, by varying the type of flexural constraint, that is, by changing from hinge to clamp, we virtually double the natural frequency of pure flexion and hence alter the ω_f/ω_t ratio.

Further, since the pure torsional frequency ω_t is usually much greater than the flexural frequency, in the clamp case ω_{fi} is closer to ω_t than it is in the hinge case. For this reason the vibrations of clamped beams have an appreciably greater flexural-torsional coupling than in the case for beams with a flexural hinge.

On the basis of the results of the study conducted on flexural-torsional vibrations we have been able to explain the rise in the first natural frequency with an appreciable flexural component observed experimentally [2] in T beams fixed at the ends, a phenomenon that could not otherwise be explained since in the experimental tests, because of a possible yielding of the constraints, it is

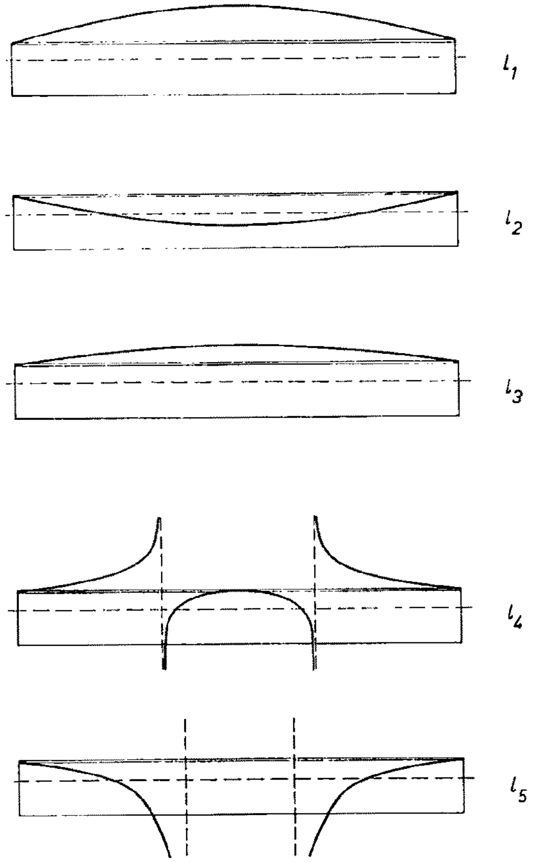

Fig. 8 - Position of the torsion center for the various modes of vibration shown in Fig. 6.

usual to measure natural frequencies lower than those calculated for a perfect joint. This rise was due to the fact that for the beams examined experimentally the first natural frequency for pure torsion was between the frequencies ω_{fi} and ω_{ti} and so, being comparable, fell into situation *c*). In particular, in the case of the fixed joint, since ω_{fi} is greater than ω_t, the first natural flexural frequency is appreciably greater than ω_{fi}. For the T beam of table 1 this situation occurs for lengths of under 5 m, length for which $\omega_{fi} \cong \omega_t$.

The calculations for flexural-torsional vibrations of beams constrained at the ends by flexural hinges and torsional clamps reached by the transfer matrix method are in good agreement with those of other authors [8] who solved the system of differential equations (1.1) by imposing sinusoidal solutions and hence valid only for the type of constraint just quoted.

6. Conclusions.

The method of calculation devised can be used for determining the natural frequencies and corresponding deformations of thin-walled open beams, that do not present warping rigidity, for any constraint condition and gives results that agree well with those obtained experimentally.

The study was carried out for T beams in particular. For this type of beam the ratio between the frequency of pure flexion ω_f and that of pure torsion ω_t was observed to have a considerable influence on the type of flexural-torsional coupling.

We would stress that the determination of the first natural frequency without allowance for flexural-torsional coupling is accurate virtually only when the first pure torsional frequency is much greater than the first pure flexural frequency.

When ω_f is comparable to or greater than ω_t, the natural frequencies calculated without taking the flexural-torsional coupling into account differ, sometimes considerably, from the actual frequencies. In any case, if ω_f is greater than ω_t, the frequency of the first mainly flexural mode is greater than ω_f and that of the mainly torsional mode is less than ω_t.

The influence of the constraints is considerable since, if the ω_f is altered, the ratio between ω_f and ω_t changes and hence, as we have seen, so do the natural flexural-torsional frequencies.

Received 8 January 1973.

REFERENCES

[1] V. Z. Vlasov, *Thin-walled elastic beams*, Israeli Program for Scientific Translations, Jerusalem 1961.
[2] A. Carpena, G. Diana, *Behaviour to wind action of angle and T bars on H. V. lattice structures*, Power apparatus and systems, no. 2, vol. 91, march-april 1972, pp. 536-544.
[3] S. P. Timoshenko, *Théorie de la flexion, torsion et flambage des barres à parois minces et à section ouverte*, L'ossature metallique, 12° anno no. 7-8, 1947.
[4] Rubinstein, *Dynamics of Structures*. Prentice-Hall, inc, Englewood Cliffs, New Jersey.
[5] K. Klotter, *Technische Schwingungslehre*, Springer Verlag, Berlin 1960.
[6] E. Pestel, F. Leckie, *Matrix methods in elastomechanics*, Mc. Graw Hill Book Co, 1963.
[7] V. Franciosi, *Scienza delle costruzioni*, ed. Liguori, Napoli 1962.
[8] E. Kosko, *The frequency spectrum of a structural member in coupled flexural-torsional vibration*, J. Sound Vib. 7 (2), 143-145, 1968.